British Journal of Pharmacology (2005) 146, 882–893
www.nature.com/bjp

Nanoparticle-induced platelet aggregation and vascular thrombosis

[1]Anna Radomski, [1]Paul Jurasz, [1]David Alonso-Escolano, [2]Magdalena Drews, [3]Maria Morandi, [2]Tadeusz Malinski & *,[1,4]Marek W. Radomski

[1]Centre for Vascular Biology, Institute of Molecular Medicine for the Prevention of Human Diseases, University of Texas Health Science Centre at Houston, 6770 Bertner Ave, Houston, TX 77025, U.S.A.; [2]Department of Biochemistry, Ohio University, Research Building 350 W. State Street; Athens, OH 45701, U.S.A.; [3]School of Public Health, University of Texas at Houston, Houston, TX, U.S.A. and [4]Silesian Centre for Heart Diseases, Szpitalna 2, 41-800 Zabrze, Poland

1 Ever increasing use of engineered carbon nanoparticles in nanopharmacology for selective imaging, sensor or drug delivery systems has increased the potential for blood platelet–nanoparticle interactions.

2 We studied the effects of engineered and combustion-derived carbon nanoparticles on human platelet aggregation *in vitro* and rat vascular thrombosis *in vivo*.

3 Multiplewall (MWNT), singlewall (SWNT) nanotubes, C60 fullerenes (C60CS) and mixed carbon nanoparticles (MCN) (0.2–300 $\mu g\,ml^{-1}$) were investigated. Nanoparticles were compared with standard urban particulate matter (SRM1648, average size 1.4 μm).

4 Platelet function was studied using lumi aggregometry, phase-contrast, immunofluorescence and transmission electron microscopy, flow cytometry, zymography and pharmacological inhibitors of platelet aggregation. Vascular thrombosis was induced by ferric chloride and the rate of thrombosis was measured, in the presence of carbon particles, with an ultrasonic flow probe.

5 Carbon particles, except C60CS, stimulated platelet aggregation (MCN $\geqslant$ SWNT > MWNT > SRM1648) and accelerated the rate of vascular thrombosis in rat carotid arteries with a similar rank order of efficacy. All particles resulted in upregulation of GPIIb/IIIa in platelets. In contrast, particles differentially affected the release of platelet granules, as well as the activity of thromboxane-, ADP, matrix metalloproteinase- and protein kinase C-dependent pathways of aggregation. Furthermore, particle-induced aggregation was inhibited by prostacyclin and *S*-nitroso-glutathione, but not by aspirin.

6 Thus, some carbon nanoparticles and microparticles have the ability to activate platelets and enhance vascular thrombosis. These observations are of importance for the pharmacological use of carbon nanoparticles and pathology of urban particulate matter.
British Journal of Pharmacology (2005) **146,** 882–893. doi:10.1038/sj.bjp.0706386;
published online 12 September 2005

Keywords: Nanoparticles; platelet aggregation; vascular thrombosis

Abbreviations: C60CS, C60 fullerenes; Gö6976, 12-(2-Cyanoethyl)-6,7,12,13-tetrahydro-13-methyl-5-oxo-5*H*-indolo(2,3-a) pyrrolo(3,4-c)-carbazole; GSNO, *S*-nitroso-glutathione; MCN, mixed carbon nanoparticles; 2-MeSAMP, 2-methylthio-AMP; MWNT, multiplewall nanotubes; SWNT, singlewall nanotubes; SRM1648, standard urban particulate matter

Introduction

The development of nanotechnology and engineered carbon nanomaterials (1–100 nm in size) greatly increased the pharmacological use of carbon and other nanoparticles. These nanoparticles have vast applications in the electronics, aerospace, computer industries, consumer products (e.g. sunscreens and cosmetics) and, more recently, in medicine (The Royal Society and Royal Academy Engineering, 2004). Indeed, the National Institutes of Health reviewing the applications of nanotechnology for monitoring, diagnosis and treatment of human diseases introduced the term of 'nanomedicine' to describe these applications (Moghimi *et al*., 2005). The delivery and targeting of pharmacological, therapeutic and diagnostic agents using nanotechnology implies the interactions of nanoparticles with blood and its elements (Winter *et al*., 2003).

There is some evidence that carbon micro-scale particles can affect vascular haemostasis and precipitate thrombosis. Indeed, personal exposure to ambient airborne particulate matter (PM) 10 μm or less in aerodynamic size diameter (PM_{10}) increased plasma fibrinogen levels (Seaton *et al*., 1999). Furthermore, peripheral thrombosis (Nemmar *et al*., 2003) has been detected following tracheal instillation of diesel exhaust particles to experimental animals. However, no data have been reported on the effects of engineered or combustion-derived nanoparticles on platelet function or vascular thrombosis.

Therefore, we investigated the effects of nanoparticles on human platelet function *in vitro* and rat vascular thrombosis. We compared the effects of nanoparticles in mixed carbon

*Author for correspondence at: 6770 Bertner Avenue, Suite C964A, Houston, TX 77030, U.S.A.;
E-mail: Marek.Radomski@uth.tmc.edu

nanoparticles (MCN), purified fullerenes (C60CS), carbon single (SWNT) and multiplewall (MWNT) open nanotubes with particles in a standard mix urban (St Louis, MS, U.S.A.) particulate matter (SRM1648, average size of 1.4 μm). For this study, we selected engineered carbon nanoparticles (C60CS, SWNT and MWNT) that are frequently used in drug discovery and delivery (LaVan *et al*., 2002; 2003), and MCN and SRM1648, which are a part of airborne PM present in the industrial environment. There is also growing concern that nanoparticles such as fullerenes, which are produced by tons each year, are accidentally released into the environment (Oberdorster, 2004). Here, we report that MCN, SWNT, MWNT, SRM1648, but not C60CS, have the ability to induce aggregation of human platelets and to enhance vascular thrombosis in rats.

Methods

Particles and reagents

Urban PM standard reference material (SRM1648) was obtained from the U.S. Department of Commerce National Institute of Standards and Technology, Gaithersburg, MD, U.S.A. MCN (a mixture of amorphous carbon with approximately 7% C60 CS), purified C60CS, purified open SWNT and MWNT were purchased from SES Research, Houston, TX, U.S.A. Particles were suspended in Tyrode's solution. In order to minimize particle self-assembly (agglomeration), particle suspensions were always sonicated for 2 min and vortexed <20 s prior to testing. In some experiments, particle suspensions were filtered through 0.1 μm filters (Millipore Corporation, U.S.A.) and the filtrate used to aggregate platelets.

12-(2-Cyanoethyl)-6,7,12,13-tetrahydro-13-methyl-5-oxo-5H-indolo(2,3-a)pyrrolo(3,4-c)-carbazole (Gö6976) was from Calbiochem (San Diego, CA, U.S.A.). Collagen and luciferin-luciferase were from Chronolog (Havertown, PA, U.S.A.). All other reagents used were purchased from Sigma-Aldrich.

Human platelets, aggregation and ATP release

Blood was obtained from healthy volunteers who had not taken any drugs known to affect platelet function for 2 weeks prior to the study. Washed platelets were isolated and resuspended in Tyrode's solution (2.5×10^8 platelets ml^{-1}), as previously described (Radomski & Moncada, 1983). Platelets were preincubated for 2 min at 37°C in a whole blood ionized calcium lumi-aggregometer (Chronolog) prior to the addition of particles (0.2–300 μg ml^{-1}). Prostacyclin (PGI_2), *S*-nitrosoglutathione (GSNO), aspirin, 2-methylthio-AMP, phenanthroline, ethylenediamine tetraacetic acid (EDTA) and Gö6976 were preincubated with platelets for 1 min before the addition of particles. Platelet aggregation was studied for 8 min and analysed using Aggro-Link data reduction system (Chronolog) (Radomski *et al*., 2001; 2002; Jurasz *et al*., 2003). The release of ATP was measured by luciferin-luciferase using lumi-aggregometer as previously described (Sawicki *et al*., 1997; Chung *et al*., 2002).

Phase-contrast, transmission electron and immunofluorescence microscopy

For phase-contrast microscopy, platelet aggregation was terminated at 20% maximal response, as determined using the aggregometer. The samples were fixed by adding an equal volume of 2% glutaraldehyde and 2% paraformaldehyde in 0.1 M phosphate buffer (PB), pH 7.4, and then incubated for 1 h at room temperature.

Aliquots of each sample were then taken for phase-contrast microscopy examination using an Olympus CKX41 microscope (Olympus America Inc., Melville, NY, U.S.A.). Photomicrographs were captured using a digital camera and MicroFire (Olympus America Inc.) software.

The remaining samples were then prepared for transmission electron microscopy examination (Alonso-Escolano *et al*., 2004). Ultrathin sections were cut in an LKB Ultracut microtome (Leica, Deerfield, IL, U.S.A.), stained with uranyl acetate and lead citrate in an LKB Ultrostainer, and examined in a JEM 1010 transmission electron microscope (JEOL Inc., Peabody, MA, U.S.A.) at an accelerating voltage of 80 kV. Digital images were obtained using the AMT Advantage digital CCD camera system (Advanced Microscopy Techniques Corp., Danvers, MA, U.S.A.).

For immunofluorescence microscopy, cytospins were prepared by centrifuging 120 μl of platelet suspension onto a glass slide in a cytocentrifuge (AC-060, Cytopro, Wescor Inc., Logan, UT, U.S.A.). Slides were allowed to air dry at room temperature and nonspecific binding was blocked by incubation for 30 min at room temperature in Dulbecco's PBS containing 10% BSA (DPBS/BSA). Slides were incubated for 60 min with anti-MMP-9 (10 μg ml^{-1}) antibodies in blocking buffer (DPBS/BSA). IgG (10 μg ml^{-1}) was used as isotype control. Following washing with DPBS/BSA, slides were incubated with a 1 : 300 dilution of anti-mouse IgG conjugated with FITC for 60 min. Following washing with PBS, the slides were mounted in SlowFade Light Antifade solution (Molecular Probes, Eugene, OR, U.S.A.) and examined using a Zeiss Axioplan 2 imaging microscope (Carl Zeiss Microimaging Inc., Thornwood, NY, U.S.A.). The immunofluorescence images were captured using AxioCam MRm digital camera (Carl Zeiss Microimaging Inc.).

The images were imported into Adobe Photoshop version 7.0 (San Jose, CA, U.S.A.), cropped and corrected for brightness and contrast, but not otherwise manipulated.

Flow cytometry

Flow cytometry was performed using a Beckman Coulter FC500 dual laser five colour flow cytometer. Flow cytometry was performed on single stained platelet samples as described previously (Jurasz *et al*., 2001; Radomski *et al*., 2001). Briefly, to minimize the presence of aggregates in samples, platelets (10 μl of suspension) and fluorescent-labelled antibodies (10 μl) containing 0.25 μg of antiactivated GPIIb/IIIa (PAC-1), anti-GPIb, anti- P-selectin (BD Biosciences, San Diego, CA, U.S.A.), or 1 μg anti-integrin β3 (SouthernBiotech, Birmingham, AL, U.S.A.) were diluted 10-fold using physiologic saline. Samples and antibodies were incubated in the dark at room temperature for 5 min. Platelets were identified by forward and side scatter signals, and 10,000 platelet-specific events were analysed by the cytometer for fluorescence.

Zymography

Zymography (Sawicki *et al*., 1997; Fernandez-Patron *et al*., 1999; Chung *et al*., 2002) was performed using 8% SDS–PAGE with copolymerized gelatin (2 mg ml^{-1}). The samples (10 μl of platelet releasate) were subjected to electrophoresis. Gels were washed in 2.5% Triton X-100 for 1 h (three times, 20 min each) and twice in zymography buffer (20 min each wash). Then, the samples were incubated in enzyme assay buffer (25 mM Tris, pH 7.5, 5 mM $CaCl_2$, 0.9% NaCl, 0.05% Na_3N) until the MMP activities could be determined. MMP-2 and MMP-9 were identified by their molecular weight and quantified by reference to purified standards (Chemicon, Temecula, CA, U.S.A.) using ChemiDoc XRS Gel Documentation System (Bio-Rad, Hercules, CA, U.S.A.) (Sawicki *et al*., 1997; Alonso-Escolano *et al*., 2004).

Rat vascular thrombosis

We used rodent ferric chloride model of carotid artery thrombosis (Kurz *et al*., 1990; Wang & Xu, 2005) with the following modifications. Wistar–Kyoto rats were anesthetized with ketamine/xylazine solution (0.09 ml 100 g^{-1} body weight) IM (thigh). The rats were placed in dorsal recumbency on a heated (37°C) surgical board. The trachea was palpated and a midline incision from the caudal end of the larynx to the suprasternal notch was made. The left carotid artery was than isolated and a Parafilm M sheet (7 × 20 mm) was placed under the carotid artery in order to prevent chloride-induced tissue damage.

To initiate thrombosis, a patch (6 × 8 mm) of micro-filter paper saturated with $FeCl_3$ solution (70% w v^{-1}) was placed on the carotid artery upstream from the flow probe. Simultaneously, a 0.5 ml suspension (50 μg ml^{-1}) of PM in 0.9% NaCl solution was injected intravenously into the femoral vein. The blood flow in carotid artery was monitored continuously with an ultrasonic flow probe (Transit Time Flowmeter TTFM Type 700, Hugo Sachs Electronik) and an in-house data-acquisition system.

Statistics

The results are expressed as mean ± s.e.m. of at least three independent experiments. Data were analysed using analysis of variance (GraphPad Prism, San Diego, CA, U.S.A.). Tukey–Kramer multiple comparisons test and Student's *t* tests were performed, where appropriate. Statistical significance was considered when $P<0.05$.

Results

Nanoparticles aggregate human platelets

Incubation of platelets with MCN, MWNT, SWNT and SRM1648, but not with C60CS, resulted in a concentration-dependent increase in platelet aggregation (Figure 1a and b). The order of efficacy was: MCN ≥ SWNT > MWNT > SRM1648 ($P<0.05$, $n=6$–10). Under these conditions, the efficacy of collagen (5 μg ml^{-1}), a physiologic aggregating agent, was similar to that of MCN (76 ± 6 *versus* 70 ± 3%, $P>0.05$, $n=8$). The aggregating ability of SRM1648 were

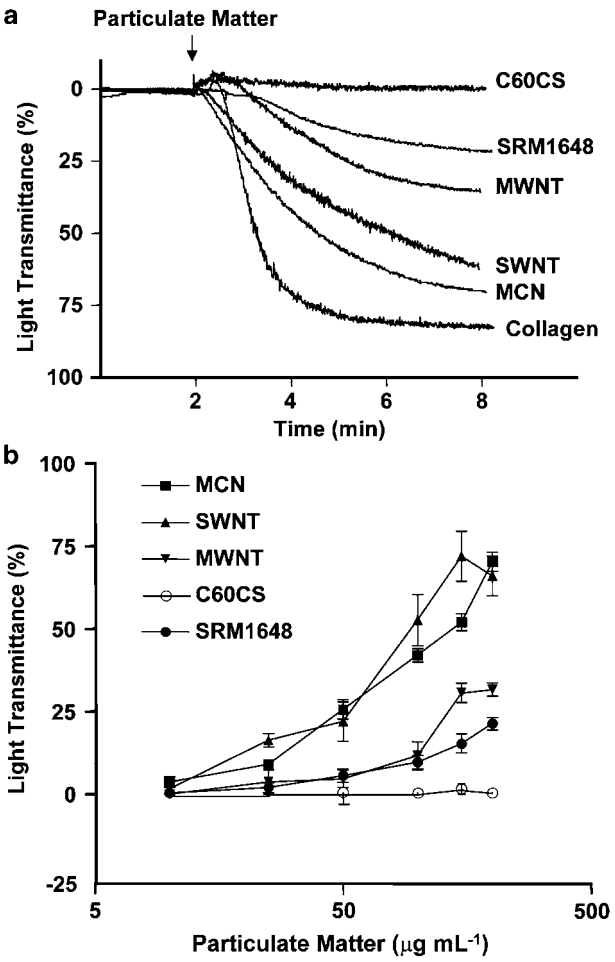

Figure 1 Aggregation of platelets by carbon nanoparticles and SRM1648. (a) Superimposed traces showing the effects of SRM1648, MCN, MWNT, SWNT and C60CS (at 200 μg ml^{-1}) on aggregation. The effect of collagen (5 μg ml^{-1}) is also shown. (b) Concentration–response curves of platelet aggregation to PM. Data are mean ± s.e.m., $n=6$–10.

abolished following filtration through 0.1 μm filter, while those of other particles was reduced by 75–85% ($n=4$). Simultaneously with aggregation, the release of ATP was investigated as an index of dense granule release (Chung *et al*., 2002). Platelets aggregated with MCN released significant amounts of ATP (1.2 ± 0.2 nM, $n=3$). In contrast, the release of ATP was not detectable (<0.1 nM, $n=3$) in platelets stimulated by the remaining types of PM.

To study closely the structure of PM-induced platelet–platelet interactions, we used phase-contrast and transmission electron microscopy. Figure 2a and b show phase-contrast control micrographs of unstimulated and collagen-aggregated platelets, respectively. The examination of platelet samples stimulated by particles revealed the presence of small (SRM1648, Figure 2c) and large (MCN and SWNT,Figure 2d and e) platelet aggregates upon incubation of platelets with particles. Incubation of platelets with C60CS did not cause aggregation (Figure 2f).

Figure 3a shows the ultrastructural appearance of unstimulated platelets. The examination of platelets aggregated with PM showed that only MCN resulted in degranulation of platelet alpha and dense granules (Figure 3c). In contrast,

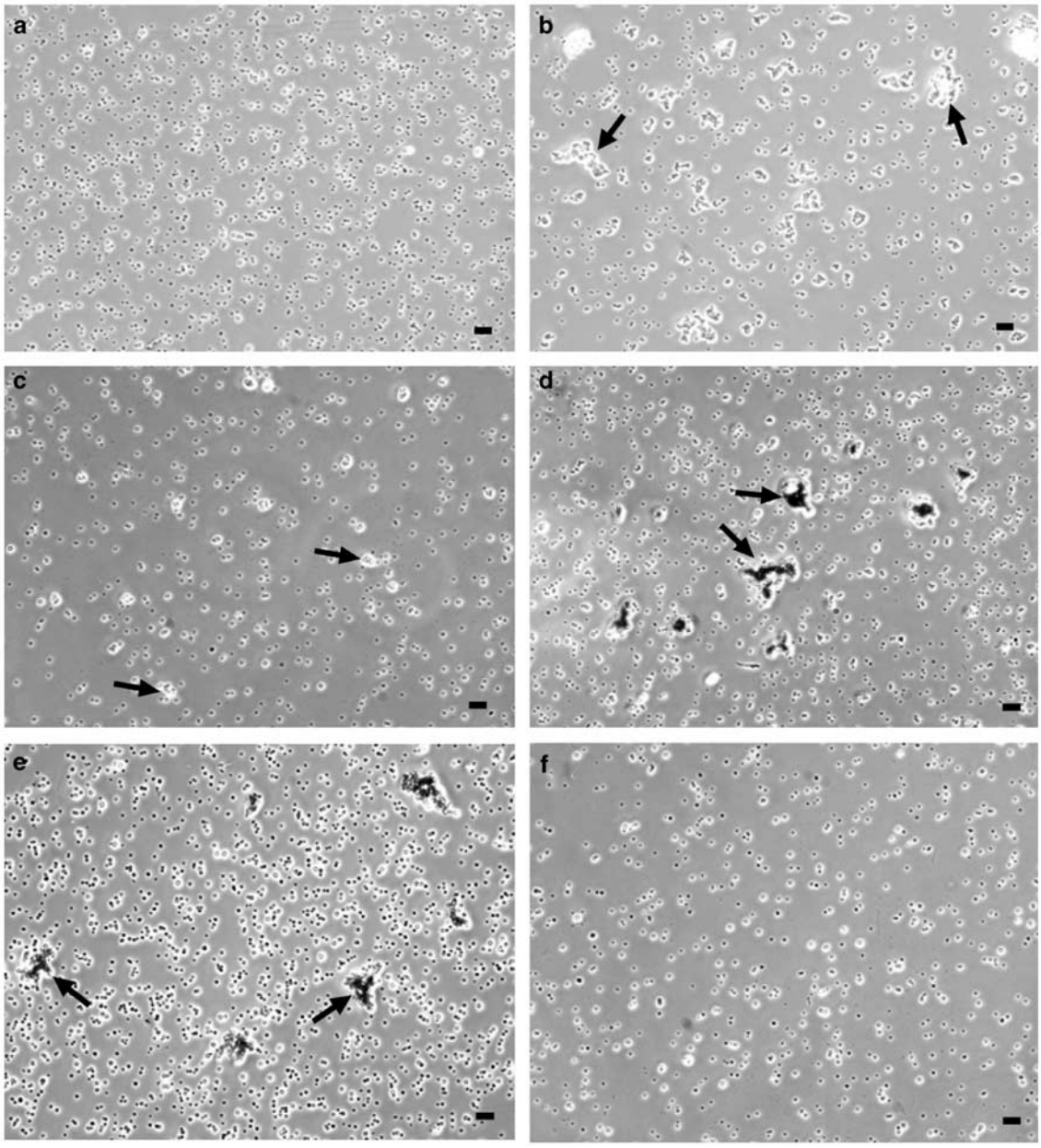

Figure 2 Phase-contrast micrographs of PM-induced aggregation. For comparison the effect of collagen ($5\,\mu g\,ml^{-1}$) is also shown. (a) Resting platelets; (b) collagen-induced aggregation; (c) SRM1648; (d) MCN; (e) SWNT; (f) C60CS. Arrows show platelet aggregates. Scale bar: $20\,\mu m$.

platelets aggregated by the remaining types of particles largely retained their granular structure; however, they showed various degree of activation, as detected by shape change, internal contractions and the extension of numerous pseudopodia (Figure 3b and d). C60CS did not result in detectable changes in platelet ultrastructure as compared to unstimulated platelets (Figure 3e). Agglomerates of particles associated with platelets were also seen in the samples of platelets aggregated with PM (Figure 4a–c). In the absence of platelets, carbon particles suspended in Tyrode's solution underwent self-assembly process and formed agglomerates sizing from 100 nm to $10\,\mu m$.

Nanoparticles amplify vascular thrombosis in rats

To confirm that the platelet-aggregating effects of nanoparticles *in vitro* could be detected *in vivo*, we studied the effects of these particles on the development of vascular thrombosis in rats. Figure 5a shows representative recordings of $FeCl_3$-induced carotid artery thrombosis and the amplifying effect of MCN on the development of thrombosis. Furthermore, infusions of MCN, SWNT and MWNT significantly accelerated time and the rate of development of carotid artery thrombosis in rats (Figure 5b). SRM1648 was less effective ($P<0.05$, $n=5$) than nanoparticles in inducing thrombosis,

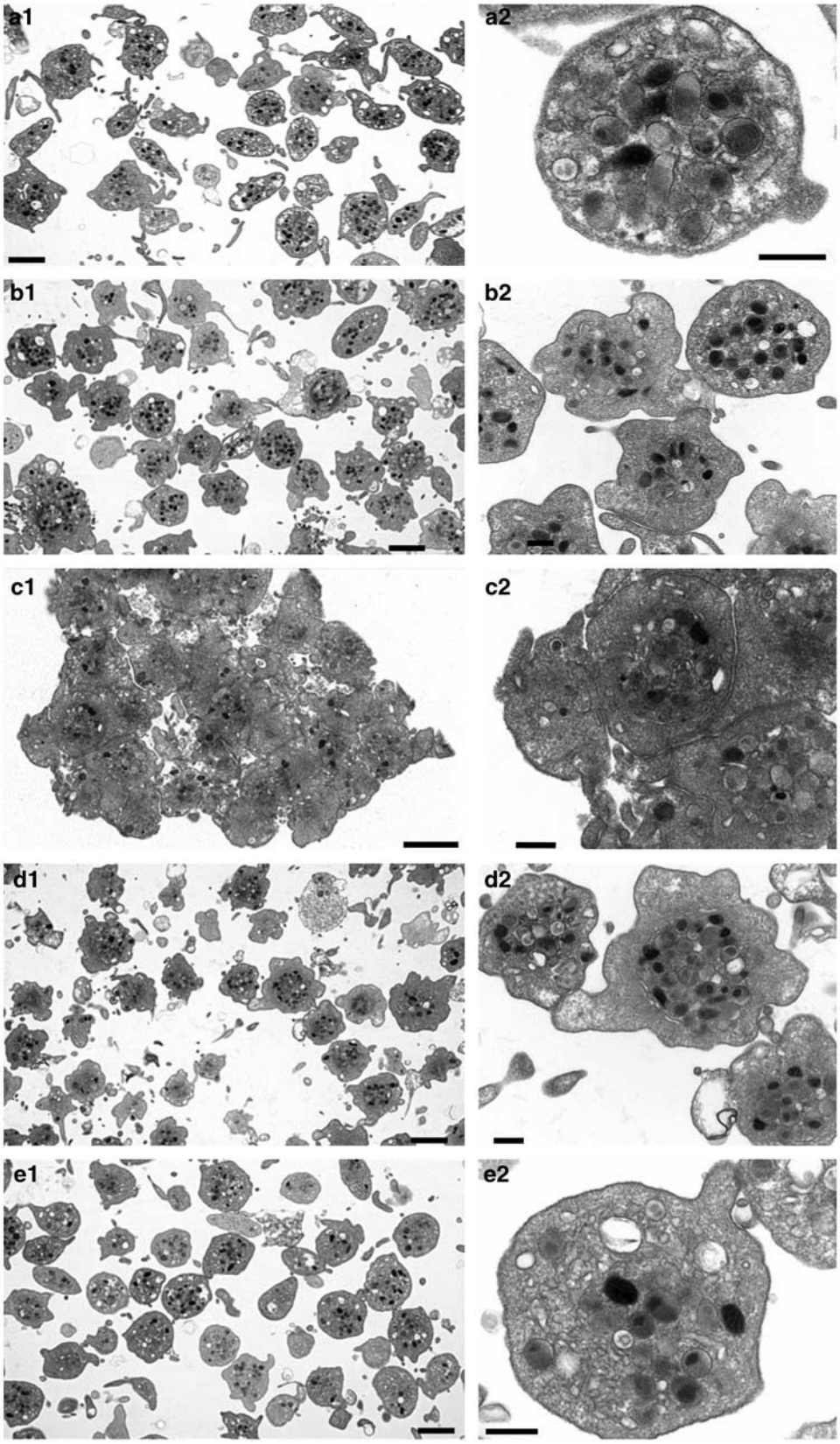

Figure 3 The ultrastructural features of PM-induced aggregation. (a) Resting platelets, (b) SRM1648, (c) MCN, (d) MWNT, (e) C60CS each at 200 $\mu g\,ml^{-1}$. (a1–e1): low-power micrographs. Note the formation of large, tight aggregate composed of mostly degranulated platelets in (c1), loose aggregates in (b1 and d1) with largely preserved granular structure and nonactivated platelets in (e1). (a2–e2) The corresponding high-power micrographs. Low-power micrographs: scale bar 2 μm; high-power micrographs: 500 nm.

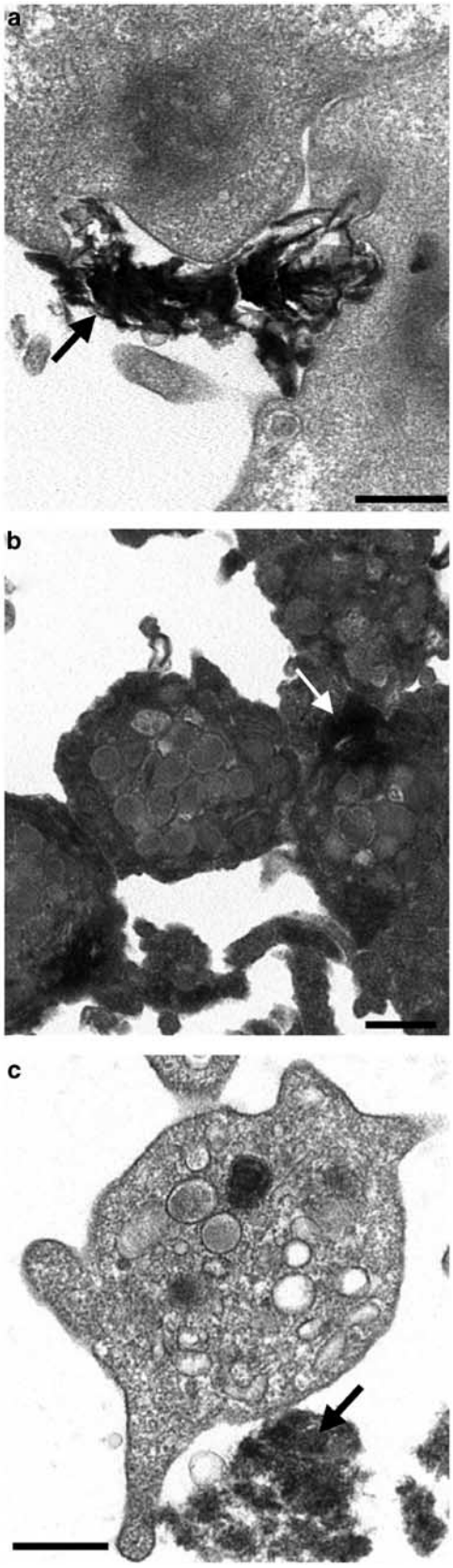

Figure 4 Association of PM agglomerates with platelets, as observed using transmission electron microscopy. (a) SRM1648; (b) MCN; (c) C60CS each at 200 μg ml^{-1}. Arrows show particle agglomerates. Scale bar: 500 nm.

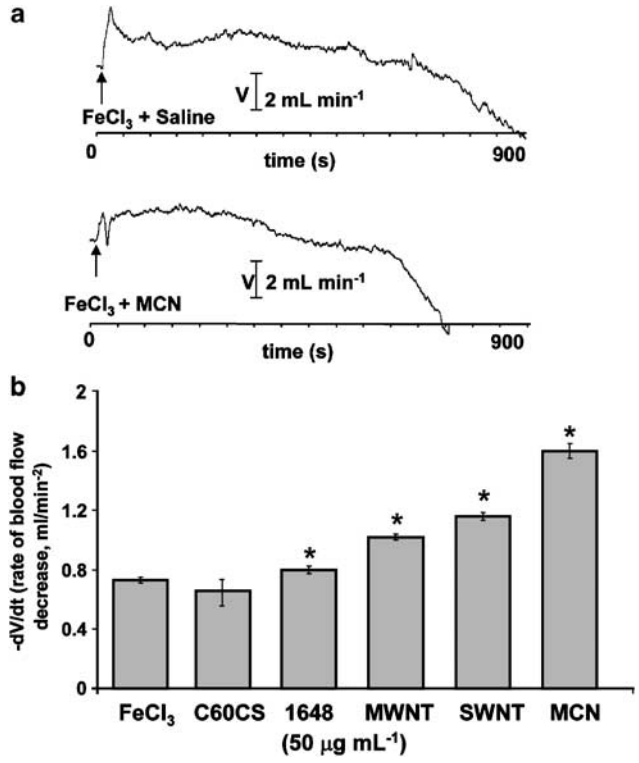

Figure 5 Stimulation of rat carotid thrombosis by nanoparticles. (a) Representative recordings showing the potentiating effect of MCN on $FeCl_3$-induced rat carotid thrombosis. (b) The rate of blood flow decreased ($-dV/dt$) by nanoparticles during $FeCl_3$-induced thrombotic occlusion of the rat carotid artery. Data are mean $\pm$ s.e.m., $n=5$. $^*P<0.05$, $FeCl_3$ + particles *versus* $FeCl_3$ + saline by ANOVA with Tukey–Kramer test.

while C60CS exerted no significant effect on the development of vascular thrombosis ($P>0.05$, $n=5$).

Mechanisms of nanoparticle-induced platelet aggregation in human platelets

Role of receptors The activation (a change from the low- to high-affinity conformation) of glycoprotein integrin receptor GPIIb/IIIa is crucial for platelet aggregation to occur (Coller, 1995). In addition, changes in the abundance of GPIb and the translocation of P-selectin from α-granules to the platelet surface membrane underlie platelet adhesion and platelet–leukocyte aggregation, respectively (Radomski & Radomski, 2000). Therefore, we measured these receptors upon aggregation with various types of particles. Figure 6a–d shows that SRM1648, MCN, MWNT and SWNT resulted in the activation of GPIIb/IIIa. The lowest concentration of MCN, which significantly increased activation of GPIIb/IIIa, was 50 μg ml^{-1} ($P<0.05$, $n=3$). The removal of extracellular divalent ions with EDTA is known to cause dissociation of GPIIb/IIIa and to inhibit its function (White & Escolar, 2000). We investigated the effect of EDTA on PM-induced aggregation. The treatment of platelets with EDTA (6 mM) resulted in complete inhibition of aggregation ($n=3$).

The treatment of platelets with MCN led to the translocation of P-selectin to the platelet surface membranes and decreased levels of GPIb (Figure 6e and f). These effects were not detected with other types of particles ($P>0.05$, $n=3$).

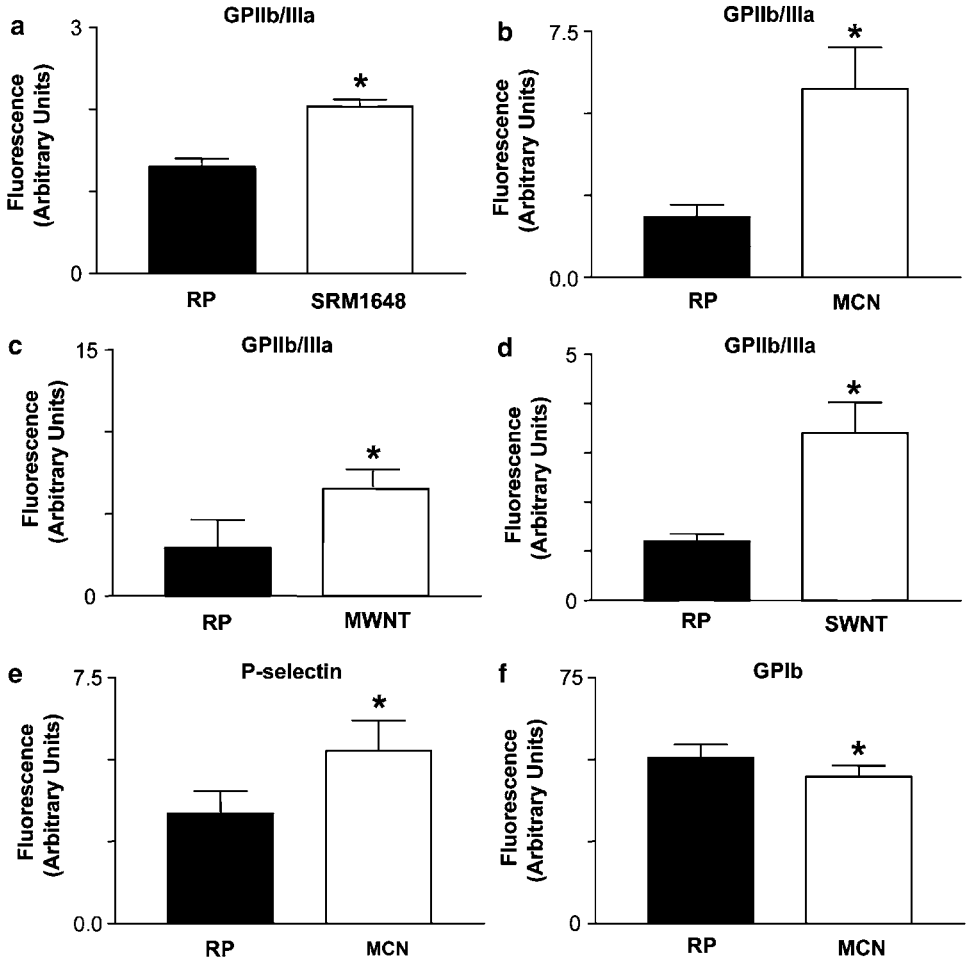

Figure 6 Effects of particles on platelet receptors. (a–d) Activation of GPIIb/IIIa by PM. (a) SRM1648; (b) MCN; (c) MWNT and (d) SWNT each at 200 μg ml^{-1}. (e and f) The effects of MCN on P-selectin and GPIb, respectively. Data are mean $\pm$ s.e.m., $n=4$. *$P<0.05$, treatments *versus* resting platelets (RP) by *t*-test.

Role of mediators and signalling pathways The activation of GPIIb/IIIa is controlled by dynamic interplay of pathways that stimulate or inhibit aggregation. Since nitric oxide (NO) and prostacyclin (PGI_2) mediate major inhibitor pathways and regulate GPIIb/IIIa function (Jurasz *et al*., 2000), we investigated the effects of PGI_2 and GSNO, an endogenous NO donor (Radomski *et al*., 1992; Stamler *et al*., 1992), on PM-induced aggregation. Both inhibitors, concentration-dependently, reduced particle-induced aggregation; however, PGI_2 was more efficacious than GSNO (Figure 7). We also studied the effects of acetylsalicylic acid (aspirin), a cyclooxygenase blocker that inhibits thromboxane A_2 (TXA_2) generation in platelets, and the most commonly used antiplatelet drug (Needleman *et al*., 1976; Vane *et al*., 1998; Awtry & Loscalzo, 2000), on aggregation stimulated by particles. Aspirin failed to affect particle-induced aggregation (Figure 7). In contrast, the same concentration of aspirin reduced collagen (5 μg ml^{-1})-induced aggregation by $65\pm8\%$ ($n=5$).

Since the release of ADP-containing dense granules was detectable during aggregation induced by MCN, we investigated the effects of 2-methylthio-AMP (2-MeSAMP), an antagonist of P2Y12 receptors, on this aggregation. The 2-MeSAMP (Alonso-Escolano *et al*., 2004), at the maximally effective concentration of 25 μM, reduced MCN (200 μg ml^{-1})-induced aggregation (from 62 ± 3 to $50\pm4\%$, $P=0.0296$, $n=3$).

The ADP- and TXA_2-signalling pathways of aggregation converge to protein kinase C (PKC), a common integrin regulator (Lévy-Toledano, 1999); therefore, we studied the actions of Gö6976 (10–1000 nM), a classical PKC isoform inhibitor (Murugappan *et al*., 2004) on PM-induced aggregation. Gö6976 inhibited collagen (5 μg ml^{-1})-induced aggregation in a concentration-dependent manner with IC_{50} of 245 ± 29 nM, $n=4$. The submaximally effective concentration of Gö6976 (300 nM) reduced aggregation stimulated with 200 μg ml^{-1} SRM1648 (from 20 ± 1 to $12\pm1\%$, $P=0.045$, $n=4$), but not with MCN, SWNT and MWNT (0–3% inhibition, $P>0.05$, $n=4$), indicating that only SRM1648 aggregates platelets in a PKC-dependent manner.

Finally, we found that phenanthroline (100 μM), which inhibits the MMP-dependent pathway of aggregation (Sawicki *et al*., 1997; Martinez-Cuesta *et al*., 2001; Radomski *et al*., 2001; Jurasz *et al*., 2002), reduced aggregation induced by SRM1648, MCN, MWNT and SWNT from 20 ± 2, 63 ± 3,

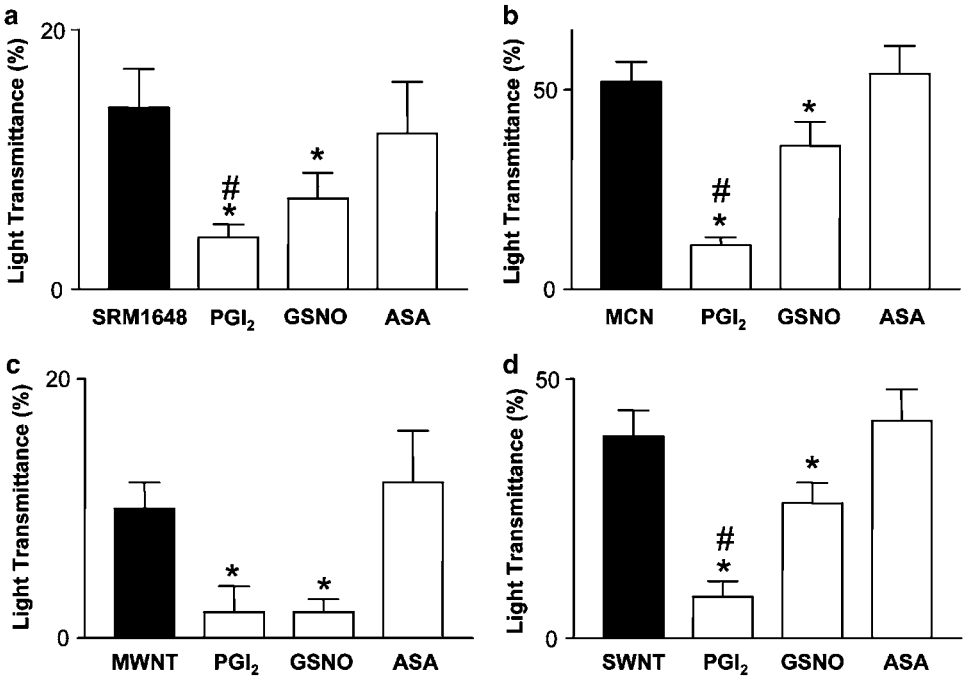

Figure 7 PM-induced aggregation is inhibited by PGI_2 (10 nM) or GSNO (10 μM), but not by aspirin (ASA, 100 μM). (a) SRM1648; (b) MCN; (c) MWNT and (d) SWNT each at 200 $\mu g\,ml^{-1}$. Data are mean$\pm$s.e.m., $n=4$. $^*P<0.05$, inhibitors *versus* PM; $^{\#}P<0.05$, GSNO *versus* PGI_2 by ANOVA with Tukey–Kramer test.

25 ± 2 and $48\pm4\%$ to 7 ± 1, 33 ± 9, 15 ± 3 and $19\pm4\%$ ($P<0.05$, $n=6$), respectively, strongly implicating platelet MMPs in the effects of PM on platelets.

Gelatinases act as stimulators (MMP-2) (Sawicki *et al*., 1997; Radomski *et al*., 2001; Alonso-Escolano *et al*., 2004) or inhibitors (MMP-9) (Fernandez-Patron *et al*., 1999; Sheu *et al*., 2004) of aggregation and their sequential release correlates with stimulation/inhibition of aggregation (Fernandez-Patron *et al*., 1999). Therefore, we studied the immunoreactivity and gelatinolytic activity of gelatinases during aggregation induced by different concentrations of PM. Figure 8a and b shows the expression of MMP-9-related immunoreactivity in platelets aggregated with SRM1648. Zymography was used to detect and quantify platelet gelatinases (Sawicki *et al*., 1997; Fernandez-Patron *et al*., 1999; Chung *et al*., 2002). Resting (nonstimulated) platelets released small amounts of these gelatinises, that is, 0.20 ± 0.05 and 0.3 ± 0.1 ng per 10^9 platelets ($n=4$) for proMMP-2 and proMMP-9, respectively. Platelet aggregation induced by PM led to a concentration-dependent release of proMMP-2 and proMMP-9 to a maximum of 2.0 ± 0.4 and 1.4 ± 0.2 ng per 10^9 platelets ($n=4$), respectively. Interestingly, particle concentrations as low as 0.2 $\mu g\,ml^{-1}$ (MCN) and 2 $\mu g\,ml^{-1}$ (SRM1648 and C60CS), which did not cause any aggregatory response, resulted in increased proMMP-9 release ($P<0.05$, $n=3$). Figure 8c shows concentration-dependent changes in the activity of these MMPs in platelets activated by PM. The highest proMMP-9/MMP-2 ratios correlated with no (C60CS) or little (lower concentrations of SRM1648, MCN, MWNT and SWNT) aggregation. Stronger aggregatory responses correlated with the increased release of MMP-2 and decreased proMMP-9/MMP-2 ratio. Table 1 summarizes the effects of nanoparticles on platelet function.

Discussion

Mechanisms of platelet activation induced by carbon nanoparticles

We found that MCN, engineered carbon nanoparticles and SRM1648 caused activation and aggregation of human platelets *in vitro*; however; there were both quantitative and qualitative differences in platelet reactivity to various types of PM. Indeed, purified C60CS did not activate platelets, SRM1648 and carbon nanotubes caused a partial aggregation with little or no granular release, while MCN resulted in platelet degranulation and the maximal aggregatory response. In this respect, the effects of MCN were similar to those of potent agonists such as large concentrations of collagen (5 $\mu g\,ml^{-1}$) or thrombin (0.1 $U\,ml^{-1}$). Interestingly, the rank-order of platelet-aggregatory efficacy of nanoparticles found in the experiments using human platelets was confirmed in a model of rat vascular thrombosis. This suggests that blood platelets are easily targeted and activated by carbon nanoparticles *in vivo*.

What mechanisms underlie interactions between nanoparticles and platelets? Nanoparticle-induced platelet aggregation is likely to result from activation of GPIIb/IIIa, as shown by flow cytometry experiments and the sensitivity of this aggregation to inhibition with EDTA, but the pathways involved in this process differ with types of particles. Platelet aggregation induced by urban-type PM (SRM1648) was inhibited by Gö6976, indicating its partial PKC dependence. In contrast, aggregation stimulated with nanoparticles appears to be PKC independent. Nanoparticle-induced aggregation was aspirin insensitive indicating that TXA_2 (if generated) did not exert significant effects on this aggregation. MCN-induced

aggregation led to ADP release. In keeping with this observation, this aggregation was reduced by antagonizing P2Y12 receptors with 2-MeSAMP. Interestingly, all types of PM tested (including nonaggregating C60CS) released gelatinases from platelets. In platelets, gelatinases are not stored in granules (Sawicki *et al*., 1998) and therefore, platelet degranulation is not the necessary prerequisite for MMP release. The activity of released MMP-2 and MMP-9 correlated with the changes in aggregation and its inhibition with phenanthroline dramatically reduced aggregation. Thus, the balance between proaggregatory MMP-2 and antiaggregatory MMP-9 (Fernandez-Patron *et al*., 1999; Sheu *et al*., 2004) plays a crucial role in PM-induced aggregation. Interestingly, the release of MMP-9 appears to be a sensitive index of cell exposure to nanoparticles of various types. Chellat *et al*. (2005) have recently demonstrated that THP-1 macrophages exposed to chitosan-DNA nanoparticles release increased amounts of MMP-9.

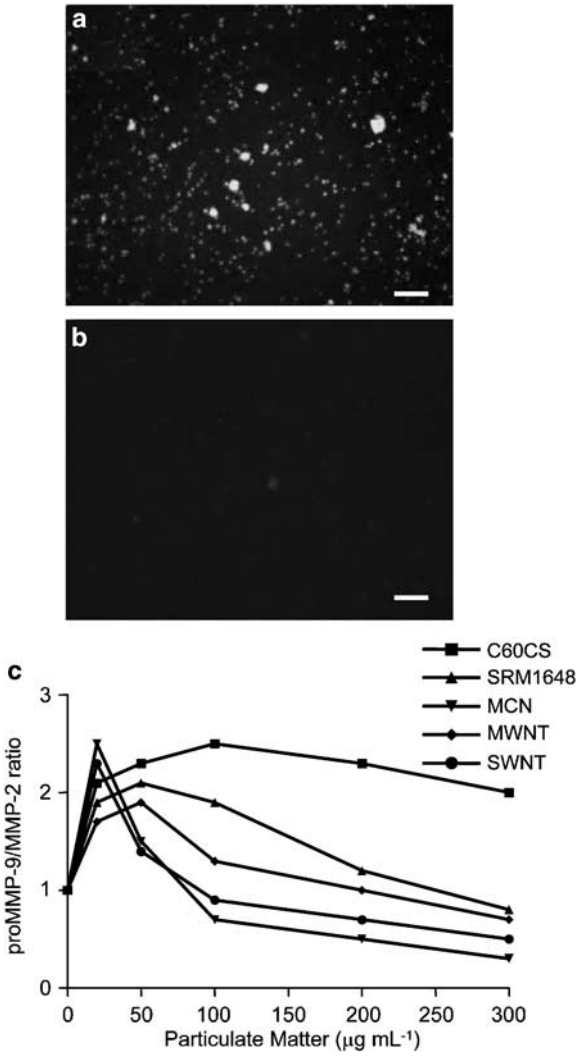

Figure 8 The immunoreactivity and activity of MMP-9 and MMP-2 during PM-induced aggregation. (a) The immunodetection of MMP-9 using anti-MMP-9 antibodies during SRM1648 ($200\,\mu g\,ml^{-1}$)-induced aggregation; (b) control IgG; (c) changes in proMMP-9/MMP-2 ratio stimulated by PM. Data points are means derived from five independent experiments. Scale bar: $20\,\mu m$.

PM-induced aggregation was inhibited by PGI_2 and GSNO demonstrating that platelets exposed to particles retain the ability to be regulated by endogenous inhibitors of vascular hemostasis.

What properties of SRM1648 and nanoparticles confer their differential potential for platelet aggregation? Although we compared the aggregatory effects of various particles in equal mass concentrations, the size of particles, their shape and surface characteristic (electrochemical charge and redox properties) are obvious considerations. Nanoparticles have a very high surface area in relation to their mass and as such are believed to be unusually reactive in their environment. In aggregation studies, some carbon nanoparticles (MCN and nanotubes) were more effective in inducing aggregation than particles of average size of $1.4\,\mu m$ (SRM1648); however, this was not the case with C60CS, which lacked the ability to aggregate platelets. Furthermore, all these particles tend to form larger (up to $10\,\mu m$) agglomerates and we observed the formation of such structures in platelet samples. This is consistent with well-known characteristics of nanoparticles such as nanotubes and C60CS that self assemble in water-based solutions (O'Connell *et al*., 2002; Richard *et al*., 2003; Burger *et al*., 2004). This process depends upon concentration of particles, it is ion dependent and may be inhibited by various surfactants and polymers (Moore *et al*., 2003). Under conditions of our experiments, all types of nanoparticles formed agglomerates; however, differential platelet reactivity to nanotubes and nanospheres does not point to a clearcut relationship between the size of agglomerates and the ability of particles to cause platelet aggregation. The second consideration is particle shape. We observed that both preparations of nanotubes (SWNT and MWNT) activated platelets, while

Table 1 Summary of carbon particle effects on platelet function

	SRM1648	*MCN*	*MWNT*	*SWNT*	*C60CS*
Aggregation *in vitro*	+	+ + +	+ +	+ +	–
Aggregation *in vivo*	+	+ + +	+ +	+ +	–
ATP release	–	+ +	–	–	–
Degranulation	–	+ +	–	–	–
GPIIb/IIIa	+	+ + +	+ +	+ +	–
PKC dependence	+	–	–	–	–
Increased MMP-9/MMP-2 ratio	–	–	–	–	+ + +
Aspirin sensitivity	–	–	–	–	–
Prostacyclin sensitivity	+ +	+ +	+ +	+ +	N/T
GSNO sensitivity	+	+	+ +	+	N/T

+/−: denotes the presence or absence of pharmacological effects; N/T: not tested.

nanospheres (C60CS) did not exert significant effects on platelet aggregation. Recently, Rustom *et al*. (2004) identified actin-tunneling nanotubes mediating cell-to-cell communication. Thus, it is possible that carbon nanotubes mimic molecular bridges involved in platelet–platelet interactions, thus stimulating aggregation, while nanospheres may not support cell–cell communication. The third consideration is particle surface. Studies showed that C60CS and nanotubes have different electrical properties and thus, surface charge (Dai, 2002). Interestingly, the binding of GPIIb/IIIa integrin to its protein ligand may depend on the multiple electrostatic interactions (Kauf *et al*., 2001). Therefore, the nanotube surface charge could play a role in direct interactions between these particles and GPIIb/IIIa. The other factor is that transition metals on the surface of particles can cause increased generation of reactive oxygen species (ROS) through the Fenton reaction (Donaldson *et al*., 2001), leading to platelet activation. Finally, the physicochemical nature of the particles (Diociaiuti *et al*., 2001) resulting from contamination with elements such as Ni and I (present in SWNT only) and multiple transition metals (in SRM1648), or the structure of the manufactured carbon nanomaterials (mostly amorphous in the case of MCN or crystal-like in the case of SWNT and MWNT) may underlie their ability to aggregate platelets. However, soluble contaminants are unlikely to be responsible for platelet activation since in our experiments the aggregating ability of particles were greatly reduced following filtration through 100 nm filters.

Significance of platelet aggregation induced by carbon nanoparticles

Our experiments using SRM1648 cast new light on the effects of urban PM on human platelet function and confirm thrombotic effects of airborne PM in animals. Indeed, Nemmar *et al*. (2003) instilled into the trachea of hamsters 5–500 μg doses of diesel exhaust particles. This dose range correlates with exposures to moderate or heavy urban pollution in megacities. The administration of diesel exhaust particles led to increased peripheral thrombosis in hamsters and correlated with the *in vitro* stimulation of platelet aggregation by these particles (Nemmar *et al*., 2003). Thus, our experiments with SRM1648 represent comparable platelet exposure to that with diesel exhaust particles. Interestingly, the personal exposure to $PM_{2.5}$ and carbon black of Danish students living in central Copenhagen led to a significant increase in platelet count and fibrinogen levels in blood (Sorensen *et al*., 2003). Taken together with observations of aggregatory effects of SRM1648 and diesel particles, these data indicate that people exposed to heightened airborne urban pollution may be at risk of developing not only atherosclerosis (Suwa *et al*., 2002) and the coronary artery disease (Peters *et al*., 2001) but also thrombotic complications of these diseases. However, prospective studies are needed to establish a clearcut link between human exposure to urban PM and the propensity for thrombosis.

Here, we report that MCN, as well as engineered purified carbon nanoparticles, share with urban-type PM the platelet-aggregatory ability. A recent survey of 27 toxicology studies have shown that, in contrast to micron-sized particles, nanomaterials can enter the body through the skin, in addition to the inhalation and oral routes (Stuart, 2003). Interestingly, studies with technetium-labelled carbon particles showed that the systemic translocation of nanosize (<100 nm) particles from the lung to peripheral blood occurs very rapidly (Nemmar *et al*., 2002). Therefore, the potential for increased systemic intake of carbon nanoparticles due to environmental exposure to nanomaterials is greater than that to the typical inhalable-size tropospheric aerosol. Furthermore, with the ever growing use of engineered nanomaterials in targeted drug delivery, biosensor or imaging systems (Buxton *et al*., 2003; Martin & Kohli, 2003), the levels of nanoparticles in blood are bound to be increased. For example, catheter-based intra-arterial local delivery of drug loaded nanoparticle agents offers a potential therapeutic approach to reducing restenosis. Local concentrations of nanoparticles required to achieve effective delivery of drug to the atherosclerotic rabbit vessel could be as high as 1 mg ml^{-1} when injected in the volume of 5 ml (Westedt *et al*., 2004) or as the 5 mg kg^{-1} dose (Kolodgie *et al*., 2002). These infusions yield calculated systemic nanoparticle levels 100 μg ml^{-1}. In our rat experiments, infusions of engineered carbon nanoparticles such as MWNT and SWNT yield calculated systemic levels 5 μg ml^{-1} leading to potentiation of vascular thrombosis. In experiments using human platelets, we studied the effects of nanoparticles on platelet aggregation measured by light aggregometry, which detected maximal aggregatory responses with concentrations of nanomaterials $\geqslant 100$ μg ml^{-1}. Using more sensitive methods such as flow cytometry (measuring activated GPIIb/IIIa) and zymography (MMP-9), we detected indices of platelet activation at concentrations of nanomaterials 4–100-fold lower than those measured by light aggregometry. For all these reasons, we believe that human platelets maybe as susceptible as rat platelets to the aggregating effects of nanoparticles.

Interestingly, some nanomaterials are clearly different than others when it comes to their platelet reactivity. Indeed, platelets are aggregated by nanotubes, but not by C60CS. Since nanotubes appear to promote cell–cell contact such as platelet aggregation, while nanospheres do not, apparently 'nonadhesive' nanomaterials such as spherical fullerenes may be preferable when designing nanopharmacological devices for targeted drug delivery or imaging systems.

Recent reports by the Royal Society and Royal Society of Engineering, as well as by the National Heart, Lung and Blood Institute Working Group on Nanotechnology have concluded that nanotechnology offers a wealth of opportunities for diagnosis and therapy of cardiovascular, pulmonary and haematological disorders (Buxton *et al*., 2003). Beyond reasonable doubt, the promise of nanotechnology and nanopharmacology cannot be overestimated. However, like with all nascent medicines and medical devices, a careful evaluation of benefits and side effects needs to be incorporated in the portfolio of applications of nanotechnology to ensure public safety and approval (The Royal Society and Royal Society of Engineering, 2004). 'The platelet compatibility' of nanomaterials may be one of such considerations.

The study was supported by the establishment grant from the University Texas-Houston to MWR. DAE was supported by a post-doctoral fellowship from the Secretaria de Estado de Educacion co-funded by the European Social Fund. The electron microscopy studies were carried out at the High Resolution Electron Microscopy Facility, UTMDACC (Institutional Core Grant #CA16672).

References

ALONSO-ESCOLANO, D., STRONGIN, A.Y., CHUNG, A.W., DERYUGINA, E.I. & RADOMSKI, M.W. (2004). Membrane type-1 matrix metalloproteinase stimulates tumour cell-induced platelet aggregation: role of receptor glycoproteins. *Br. J. Pharmacol.,* **141,** 241–252.

AWTRY, E.H. & LOSCALZO, J. (2000). Aspirin. *Circulation,* **101,** 1206–1218.

BURGER, C., HAO, J., YING, Q., ISOBE, H., SAWAMURA, M., NAKAMURA, E. & CHU, B. (2004). Multilayer vesicles and vesicle clusters formed by the fullerene-based surfactant C60(CH3)5K. *J. Colloid Interface Sci.,* **275,** 632–641.

BUXTON, D.B., LEE, S.C., WICKLINE, S.A., FERRARI, M. & FOR THE WORKING GROUP MEMBERS (2003). Recommendations of the National Heart, Lung, and Blood Institute Nanotechnology Working Group. *Circulation,* **108,** 2737–2742.

CHELLAT, F., GRANDJEAN-LAQUERRIERE, A., NAOUR, R.L., FERNANDES, J., YAHIA, L.H., GUENOUNOU, M. & LAURENT-MAQUIN, D. (2005). Metalloproteinase and cytokine production by THP-1 macrophages following exposure to chitosan-DNA nanoparticles. *Biomaterials,* **26,** 961–970.

CHUNG, A.W., JURASZ, P., HOLLENBERG, M.D. & RADOMSKI, M.W. (2002). Mechanisms of action of proteinase-activated receptor agonists on human platelets. *Br. J. Pharmacol.,* **135,** 1123–1132.

COLLER, B.S. (1995). Blockade of platelet GPIIb/IIIa receptors as an antithrombotic strategy. *Circulation,* **92,** 2373–2380.

DAI, H. (2002). Carbon nanotubes: synthesis, integration, and properties. *Accounts Chem. Res.,* **35,** 1035–1044.

DIOCIAIUTI, M., BALDUZZI, M., DE BERARDIS, B., CATTANI, G., STACCHINI, G., ZIEMACKI, G., MARCONI, A. & PAOLETTI, L. (2001). The Two PM2.5 (Fine) and PM2.5-10 (Coarse) fractions: evidence of different biological activity. *Environm. Res.,* **86,** 254–262.

DONALDSON, K., STONE, V., SEATON, A. & MACNEE, W. (2001). Ambient particle inhalation and the cardiovascular system: potential mechanisms. *Environm. Health Perspect.,* **109** (Suppl. 4), 523–527.

FERNANDEZ-PATRON, C., MARTINEZ-CUESTA, M.A., SALAS, E., SAWICKI, G., WOZNIAK, M., RADOMSKI, M.W. & DAVIDGE, S.T. (1999). Differential regulation of platelet aggregation by matrix metalloproteinases-9 and -2. *Thromb. Haemostasis,* **82,** 1730–1735.

JURASZ, P., ALONSO, D., CASTRO_BLANCO, S., MURAD, F. & RADOMSKI, M.W. (2003). Generation and role of angiostatin in human platelets. *Blood,* **102,** 3217–3223.

JURASZ, P., CHUNG, A.W., RADOMSKI, A. & RADOMSKI, M.W. (2002). Nonremodeling properties of matrix metalloproteinases: the platelet connection. *Circulat. Res. (online),* **90,** 1041–1043.

JURASZ, P., RADOMSKI, A., SAWICKI, G., MAYERS, I. & RADOMSKI, M.W. (2000). Nitric oxide and platelet function. In: *Nitric oxide Biol. Pathobiol.,* ed. Ignarro, L.J., pp. 823–840. San Diego, San Francisco, New York, Boston, Sydney, Tokyo: Academic Press.

JURASZ, P., STEWART, M.W., RADOMSKI, A., KHADOUR, F., DUSZYK, M. & RADOMSKI, M.W. (2001). Role of von Willebrand factor in tumour cell-induced platelet aggregation: differential regulation by NO and prostacyclin. *Br. J. Pharmacol.,* **134,** 1104–1112.

KAUF, A.C.W., HOUGH, S.M. & BOWDITCH, R.D. (2001). Recognition of fibronectin by the platelet integrin IIb3 involves an extended interface with multiple electrostatic interactions. *Biochemistry,* **40,** 915–9166.

KOLODGIE, F.D., JOHN, M., KHURANA, C., FARB, A., WILSON, P.S., ACAMPADO, E., DESAI, N., SOON-SHIONG, P. & VIRMANI, R. (2002). Sustained reduction of in-stent neointimal growth with the use of a novel systemic nanoparticle paclitaxel. *Circulation,* **106,** 1195–1198.

KURZ, K.D., MAIN, B.W. & SANDUSKY, G.E. (1990). Rat model of arterial thrombosis induced by ferric chloride. *Thromb. Res.,* **60,** 269–280.

LAVAN, D.A., LYNN, D.M. & LANGER, R. (2002). Moving smaller in drug discovery and delivery. *Nat. Rev. Drug Discov.,* **1,** 77–84.

LAVAN, D.A., MCGUIRE, T. & LANGER, R. (2003). Small-scale systems for *in vivo* drug delivery. *Nat. Biotechnol.,* **21,** 1184–1191.

LÉVY-TOLEDANO, S. (1999). Platelet signal transduction pathways: could we organize them into a 'hierarchy'? *Pathophysiol. Haemostasis Thromb.,* **29,** 4–15.

MARTIN, C.R. & KOHLI, P. (2003). The emerging field of nanotube biotechnology. *Nat. Rev. Drug Discov.,* **2,** 29–37.

MARTINEZ-CUESTA, M.A., SALAS, E., RADOMSKI, A. & RADOMSKI, M.W. (2001). Matrix metalloproteinase-2 in platelet adhesion to fibrinogen: interactions with nitric oxide. *Med. Sci. Monit.,* **7,** 646–651.

MOGHIMI, S.M., HUNTER, A.C. & MURRAY, J.C. (2005). Nanomedicine: current status and future prospects. *FASEB J.,* **19,** 311–330.

MOORE, V.C., STRANO, M.S., HAROZ, E.H., HAUGE, R.H. & SMALLEY, R.E. (2003). Individually suspended single-walled carbon nanotubes in various surfactants. *Nanoletters,* **3,** 1379–1382.

MURUGAPPAN, S., TULUC, F., DORSAM, R.T., SHANKAR, H. & KUNAPULI, S.P. (2004). Differential role of protein kinase C{delta} isoform in agonist-induced dense granule secretion in human platelets. *J. Biol. Chem.,* **279,** 2360–2367.

NEEDLEMAN, P., MONCADA, S., BUNTING, S., VANE, J.R., HAMBERG, M. & SAMUELSSON, B. (1976). Identification of an enzyme in platelet microsomes which generates thromboxane A2 from prostaglandin endoperoxides. *Nature,* **261,** 558–560.

NEMMAR, A., HOET, P.H.M., DINSDALE, D., VERMYLEN, J., HOYLAERTS, M.F. & NEMERY, B. (2003). Diesel exhaust particles in lung acutely enhance experimental peripheral thrombosis. *Circulation,* **107,** 1202–1208.

NEMMAR, A., HOET, P.H.M., VANQUICKENBORNE, B., DINSDALE, D., THOMEER, M., HOYLAERTS, M.F., VANBILLOEN, H., MORTELMANS, L. & NEMERY, B. (2002). Passage of inhaled particles into the blood circulation in humans. *Circulation,* **105,** 411–414.

OBERDORSTER, E. (2004). Manufactured nanomaterials (fullerenes, C60) induce oxidative stress in the brain of juvenile largemouth bass. *Environm. Health Perspect.,* **112,** 1058–1062.

O'CONNELL, M.J., BACHILO, S.M., HUFFMAN, C.B., MOORE, V.C., STRANO, M.S., HAROZ, E.H., RIALON, K.L., BOUL, P.J., NOON, W.H., KITTRELL, C., MA, J., HAUGE, R.H., WEISMAN, R.B. & SMALLEY, R.E. (2002). Band gap fluorescence from individual single-walled carbon nanotubes. *Science,* **297,** 593–596.

PETERS, A., DOCKERY, D.W., MULLER, J.E. & MITTLEMAN, M.A. (2001). Increased particulate air pollution and the triggering of myocardial infarction. *Circulation,* **103,** 2810–2815.

RADOMSKI, A., JURASZ, P., SANDERS, E.J., OVERALL, C.M., BIGG, H.F., EDWARDS, D.R. & RADOMSKI, M.W. (2002). Identification, regulation and role of tissue inhibitor of metalloproteinases-4 (TIMP-4) in human platelets. *Br. J. Pharmacol.,* **137,** 1330–1338.

RADOMSKI, A., STEWART, M.W., JURASZ, P. & RADOMSKI, M.W. (2001). Pharmacological characteristics of solid-phase von Willebrand factor in human platelets. *Br. J. Pharmacol.,* **134,** 1013–1020.

RADOMSKI, M. & MONCADA, S. (1983). An improved method for washing of human platelets with prostacyclin. *Thromb. Res.,* **30,** 383–389.

RADOMSKI, M.W. & RADOMSKI, A.S. (2000). Regulation of blood cell function by the endothelial cells. In: *Vascular Endothelium in Human Physiology and Pathophysiology,* eds. Vallance, P. & Webb, D. pp. 95–106. London: Harwood Academic Publishers.

RADOMSKI, M.W., REES, D.D., DUTRA, A. & MONCADA, S. (1992). *S*-nitroso-glutathione inhibits platelet activation *in vitro* and *in vivo*. *Br. J. Pharmacol.,* **107,** 745–749.

RICHARD, C., BALAVOINE, F., SCHULTZ, P., EBBESEN, T.W. & MIOSKOWSKI, C. (2003). Supramolecular self-assembly of lipid derivatives on carbon nanotubes. *Science,* **300,** 775–778.

RUSTOM, A., SAFFRICH, R., MARKOVIC, I., WALTHER, P. & GERDES, H.-H. (2004). Nanotubular highways for intercellular organelle transport. *Science,* **303,** 1007–1010.

SAWICKI, G., SALAS, E., MURAT, J., MISZTA_LANE, H. & RADOMSKI, M.W. (1997). Release of gelatinase A during platelet activation mediates aggregation. *Nature,* **386,** 616–619.

SAWICKI, G., SANDERS, E.J., SALAS, E., WOZNIAK, M., RODRIGO, J. & RADOMSKI, M.W. (1998). Localization and translocation of MMP-2 during aggregation of human platelets. *Thromb. Haemostasis,* **80,** 836–839.

SEATON, A., SOUTAR, A., CRAWFORD, V., ELTON, R., MCNERLAN, S., CHERRIE, J., WATT, M., AGIUS, R. & STOUT, R. (1999). Particulate air pollution and the blood. *Thorax,* **54,** 1027–1032.

SHEU, J.R., FONG, T.H., LIU, C.M., SHEN, M.Y., CHEN, T.L., CHANG, Y., LU, M.S. & HSIAO, G. (2004). Expression of matrix metalloproteinase-9 in human platelets: regulation of platelet activation in *in vitro* and *in vivo* studies. *Br. J. Pharmacol.,* **143,** 193–201.

SORENSEN, M., DANESHVAR, B., HANSEN, M., DRAGSTED, L.O., HERTEL, O., KNUDSEN, L. & LOFT, S. (2003). Personal PM2.5 exposure and markers of oxidative stress in blood. *Environm. Health Perspect.,* **111,** 161–166.

STAMLER, J., JARAKI, O., OSBORNE, J., SIMON, D., KEANEY, J., VITA, J., SINGEL, D., VALERI, C. & LOSCALZO, J. (1992). Nitric oxide circulates in mammalian plasma primarily as an *S*-nitroso adduct of serum albumin. *Proc. Natl. Acad. Sci. U.S.A.,* **89,** 7674–7677.

STUART, C. (2003). Survey finds the smaller in size, the bigger the possible risks. URL: http://www.smalltimes.com/document_display.cfm?document_id = 5861.

SUWA, T., HOGG, J.C., QUINLAN, K.B., OHGAMI, A., VINCENT, R. & VAN EEDEN, S.F. (2002). Particulate air pollution induces progression of atherosclerosis. *J. Am. College Cardiol.,* **39,** 935–942.

THE ROYAL SOCIETY AND ROYAL ACADEMY OF ENGINEERING (2004). *Nanoscience and nanotechnology: opportunities and uncertainties*, http://www.nanotec.org.uk/finalReport.htm.

VANE, J.R., BAKHLE, Y.S. & BOTTING, R.M. (1998). Cyclooxygenases 1 and 2. *Annu. Rev. Pharmacol. Toxicol.,* **38,** 97–120.

WANG, X. & XU, L. (2005). An optimized murine model of ferric chloride-induced arterial thrombosis for thrombosis research. *Thromb. Res.,* **115,** 95–100.

WESTEDT, U., BARBU-TUDORAN, L., SCHAPER, A.K., KALINOWSKI, M., ALFKE, H. & KISSEL, T. (2004). Effects of different application parameters on penetration characteristics and arterial vessel wall integrity after local nanoparticle delivery using a porous balloon catheter. *Eur. J. Pharm. Biopharm.,* **58,** 161–168.

WHITE, J.G. & ESCOLAR, G. (2000). EDTA-induced changes in platelet structure and function: adhesion and spreading. *Platelets,* **11,** 56–61.

WINTER, P.M., MORAWSKI, A.M., CARUTHERS, S.D., FUHRHOP, R.W., ZHANG, H., WILLIAMS, T.A., ALLEN, J.S., LACY, E.K., ROBERTSON, J.D., LANZA, G.M. & WICKLINE, S.A. (2003). Molecular imaging of angiogenesis in early-stage atherosclerosis with {alpha}v{beta}3-integrin-targeted nanoparticles. *Circulation,* **108,** 2270–2274.

(Received June 16, 2005
Accepted August 4, 2005
Published online 12 September 2005)